EURASIP Journal on Advances in Signal Processing
a SpringerOpen Journal

RESEARCH Open Access

Performance analysis of OFDM modulation on indoor broadband PLC channels

José Antonio Cortés*, Luis Díez, Francisco Javier Cañete, Juan José Sánchez-Martínez and José Tomás Entrambasaguas

Abstract

Indoor broadband power-line communications is a suitable technology for home networking applications. In this context, orthogonal frequency-division multiplexing (OFDM) is the most widespread modulation technique. It has recently been adopted by the ITU-T Recommendation G.9960 and is also used by most of the commercial systems, whose number of carriers has gone from about 100 to a few thousands in less than a decade. However, indoor power-line channels are frequency-selective and exhibit periodic time variations. Hence, increasing the number of carriers does not always improves the performance, since it reduces the distortion because of the frequency selectivity, but increases the one caused by the channel time variation. In addition, the long impulse response of power-line channels obliges to use an insufficient cyclic prefix. Increasing its value reduces the distortion, but also the symbol rate. Therefore, there are optimum values for both modulation parameters. This article evaluates the performance of an OFDM system as a function of the number of carriers and the cyclic prefix length, determining their most appropriate values for the indoor power-line scenario. This task must be accomplished by means of time-consuming simulations employing a linear time-varying filtering, since no consensus on a tractable statistical channel model has been reached yet. However, this study presents a simpler procedure in which the distortion because of the frequency selectivity is computed using a time-invariant channel response, and an analytical expression is derived for the one caused by the channel time variation.

1. Introduction

The increasing demand for home networking capabilities has attracted considerable interest to high-speed indoor power-line communications (PLC). Despite this technology is able to provide the data rates required by the most common in-home applications, the lack of an international technical standard has traditionally restrained its deployment. However, this situation is expected to change with the upcoming International Telecommunication Union (ITU) Recommendation G.9960 [1,2]. In fact, several telecom operators are now using PLC devices to carry the signals of their triple-play services from the gateway to the set-top box.

At this moment, the available bandwidth for broadband indoor PLC applications extends up to 30 MHz [3]. Communication channels in this band are frequency and time-selective, with remarkable disparity even among different locations in a specific site [4]. Time variations have a twofold origin: long-term changes because of the connection or disconnection of electrical devices, and short-term changes caused by the time-variant behavior of the impedance and the noise emitted by the electrical devices [5]. The former has no interest for this study, since the time between consecutive transitions, after which a new channel appears, is in the order of minutes or hours. The latter has a periodical nature, which allows the channel to be modeled by means of a linear periodically time-varying (LPTV) filter plus an additive cyclostationary-colored noise term [5].

Orthogonal frequency-division multiplexing (OFDM) is a suitable technique to cope with these channel impairments. In fact, it has been adopted by the ITU-T Rec. G.9960 and by most PLC commercial systems. The latter have increased their data rates from about 10 Mbit/s up to more than 100 Mbit/s in less than one decade. Part of this improvement is because of the increment in the number of carriers, which has gone from about 100 up to a few thousands, and in the cyclic

* Correspondence: jaca@ic.uma.es
Departamento de Ingeniería de Comunicaciones, Escuela Técnica Superior de Ingeniería de Telecomunicación, Universidad de Málaga, Málaga, Spain

prefix length, which has gone from about 3.3 up to 5.6 μs [6,7]. However, these values seem to be driven by an implementation complexity criterion rather than by an optimality one, since performance studies accomplished up to now have not considered the channel time variation effect [8,9].

When an OFDM signal traverses a frequency-selective time-varying channel, two distortion components appear: the frequency selectivity causes intersymbol interference (ISI) and intercarrier interference (ICI), while the channel time variation results in ICI [10]. Increasing the number of carriers reduces the distortion caused by the frequency selectivity of the channel and improves the transmission efficiency, because the duration of the cyclic prefix represents a smaller percentage of the overall symbol length. On the other hand, it enlarges the symbol length, increasing the ICI because of the channel time variation [11]. Thus, if the number of carriers is too low (or too high), the distortion due to the frequency selectivity (or to the channel time variation) may be greater than the noise, and the performance is limited by an improper number of carriers. Regarding the cyclic prefix, increasing its length reduces the distortion caused by the frequency selectivity of the channel, but decreases the symbol rate. Hence, enlarging the cyclic prefix improves the data rate only if the power of the remaining distortion due to the frequency selectivity stays much greater than the noise and the distortion caused by the channel time variation. Once the contribution of the latter terms dominates, lengthening the cyclic prefix is counterproductive because the OFDM symbol rate is reduced without profit [12]. Therefore, there exist optimum values for both the number of carriers and the cyclic prefix length.

The performance of OFDM has largely been investigated in the mobile radio environment. In this scenario, channel impulse responses are quite short (compared to the symbol length). Hence, the optimum value for the cyclic prefix length is equal to the duration of the channel impulse response. This eliminates the distortion due to the frequency selectivity, and makes the ICI due to the channel time variation the key element of the optimization problem. The optimization is usually accomplished in terms of the signal-to-interference ratio (SIR), or the signal-to-noise and interference ratio (SNIR) [13]. However, obtaining a closed-form expression for the ICI can be difficult in some channel models [14]. Therefore, approximate expressions are usually derived by assuming that the channel variation along the OFDM symbol is linear [13,15,16].

The aforementioned study is not applicable to indoor PLC scenarios, where there is no agreement on a statistical channel model and bottom-up (deterministic) approaches seem to be more appropriate [17,18]. This fact has an important implication: it is impossible to draw closed-form expressions for the ICI, the SNIR, or the probability distribution of the ICI. Hence, distortion terms can only be estimated by means of time-consuming LPTV simulations accomplished over a set of measured or bottom-up modeled channels. Moreover, the long impulse response of PLC channels obliges to use an insufficient cyclic prefix, which makes the distortion caused by the frequency selectivity to be also present. As a consequence, maximizing the SNIR no longer maximizes the data rate, as it happens in the mobile radio case.

In this context, we make two main contributions:

- We propose a fast and simple method to compute the overall distortion suffered by an OFDM signal over an indoor power-line channel. The ISI and ICI due to the frequency selectivity are computed using a linear time-invariant (LTI) channel. This procedure is grounded on the observation that the delay spread, which is the responsible for these distortion components, is almost time-invariant [19]. To calculate the ICI caused by the channel time variation, we derive an analytical expression, which adopts a particularly compact form because of the periodic behavior of the channel response.
- We evaluate the performance of broadband OFDM systems on indoor power-line channels as a function of the number of carriers and the cyclic prefix length. Obtained results allow assessing the suitability of the parameters currently employed by commercial systems.

The rest of the article is organized as follows. Section 2 describes the channel model. Section 3 presents the employed OFDM system model and the method proposed to compute the distortion terms, which is validated in Section 4. The proposed procedure is used in Section 5 to evaluate the performance of the OFDM modulation. Main conclusions are summarized in Section 6.

2. Channel model

In most countries, indoor power networks have a branched structure composed of a set of wires with different sections and ended in open circuits or in connected appliances. Since impedances presented by the appliances are quite diverse, the injected signal experiences multipath propagation. More than the link distance, the relevant factors in the frequency selectivity are the number of branches and their relative situation, lengths, and loads [4]. In addition, the channel behavior exhibits a short-term variation, synchronous with the mains, due to the dependence of the impedance presented by the electrical devices on the mains voltage [5].

Noise in the indoor power-line environment is mainly generated by the electrical devices connected to the power grid, although external noise sources are also coupled to the indoor network via radiation or via conduction. It is composed of three major terms: narrowband interferences, impulsive noise, and background noise. The former can be assumed stationary, and the latter can be modeled by means of a Gaussian cyclostationary-colored process [20].

In this article, it is assumed that the working state of the electrical devices remains unaltered and no impulsive noise components are present. Under these circumstances, the channel can be modeled as an LPTV system plus a cyclostationary Gaussian noise term [20]. However, at this time there are no accepted statistical models neither for the LPTV channel response nor for the cyclostationary-colored noise. The only alternatives to obtain the LPTV responses are either to use deterministic models to generate an ensemble of channels [21] or to use a set of measured channels. Regarding the noise, the only possibility is to generate it according to instantaneous power spectral densities (IPSD) drawn from measurements.

This study uses a set of more than 50 LPTV channel responses and noise IPSD measured in three different locations in the frequency band from 1 up to 20 MHz. A detailed characterization of both elements can be found in [5]. However, for the sake of clarity, the qualitative features of the method proposed to evaluate the distortion are illustrated using only one of the aforementioned channels. It has been selected because of the significant time variation of its channel response. In the mobile radio environment, this variation is due to the Doppler effect and is quantified by means of the so-called Doppler spread [22]. In power-line scenarios, time variation is caused by the electrical devices and exhibits a periodical behavior with harmonics of the mains frequency, f_0, which is 50 Hz in Europe. Hence, the channel frequency response, $H(t, f)$, can be expanded as a Fourier Series,

$$H(t,f) = \sum_{\alpha=-\infty}^{\infty} H^{\alpha}(f) e^{-j2\pi f_0 \alpha t}. \quad (1)$$

A sort of Doppler spread, $B_D(f)$, can then be defined as the largest nonzero Fourier series coefficient. In practice, $H(t, f)$ is obtained from real measurements and $H^{\alpha}(f)$ is non-zero for all the values of α. In these cases, the Doppler spread can be computed as $B_D(f) = \alpha_L f_0$, where α_L is the largest coefficient for which $H^{\alpha}(f)$ has reduced 40 dB below its maximum, $H^0(f)$ [5]. Figure 1a, b depicts the time-averaged power delay profile (PDP) and the Doppler spread values of the selected channel. The quantized nature of $B_D(f)$ at multiples of f_0 is observable in Figure 1b.

The frequency selectivity of the selected channel can be clearly seen in Figure 2a, where the averaged value of the channel attenuation along the mains period, $T_0 = 1/f_0$,

$$|H(f)| = \frac{1}{T_0} \int_{-\frac{T_0}{2}}^{\frac{T_0}{2}} |H(t,f)|\, dt, \quad (2)$$

has been depicted. Similarly, the magnitude of the time variations is clear in Figure 2b, where the time evolution of the amplitude response along the mains cycle at two frequencies is shown. As seen, there are frequency bands with more than 6 dB of amplitude variation.

3. Distortion evaluation

This section describes a method for the computation of the distortion caused by the frequency selectivity and the time variation of the channel response. Hence, no noise is considered in the analysis.

The discrete-time expression of a baseband OFDM signal with N carriers and cp samples of cyclic prefix is given by

$$x[n] = \frac{1}{N} \sum_{q=-\infty}^{\infty} \sum_{i=-N/2+1}^{N/2} X_{q,i} e^{j\frac{2\pi}{N} i(n-cp-qL)} w[n-qL], \quad (3)$$

where $L = N + cp$ is the symbol length, $X_{q,\,i}$ is the qth data symbol transmitted in carrier i and $w[n]$ is a rectangular window with non-zero samples in the range $0 \le n \le L - 1$.

Let us consider an indoor power-line channel sampled with a frequency that is a large multiple of the mains one. Its baseband equivalent impulse response can be expressed as $h[n, m]$, where n is the observation time and $n - m$ is the time at which the impulse is applied. The channel output to the input signal $x[n]$ can be expressed as [23]

$$y[n] = \sum_{m=0}^{L_h(n)-1} h[n,m] x[n-m], \quad (4)$$

where $L_h(n)$ is the length of the impulse response at time n. However, as measurements indicate that $L_h(n)$ is essentially invariant along the mains cycle [19], from now on it is denoted by L_h.

At the receiver, the output of the DFT in carrier k for the ℓth transmitted symbol can be expressed as

$$Y_{\ell,k} = \sum_{n=0}^{N-1} y[n + \ell L + cp + D] e^{-j\frac{2\pi}{N} kn}, \quad (5)$$

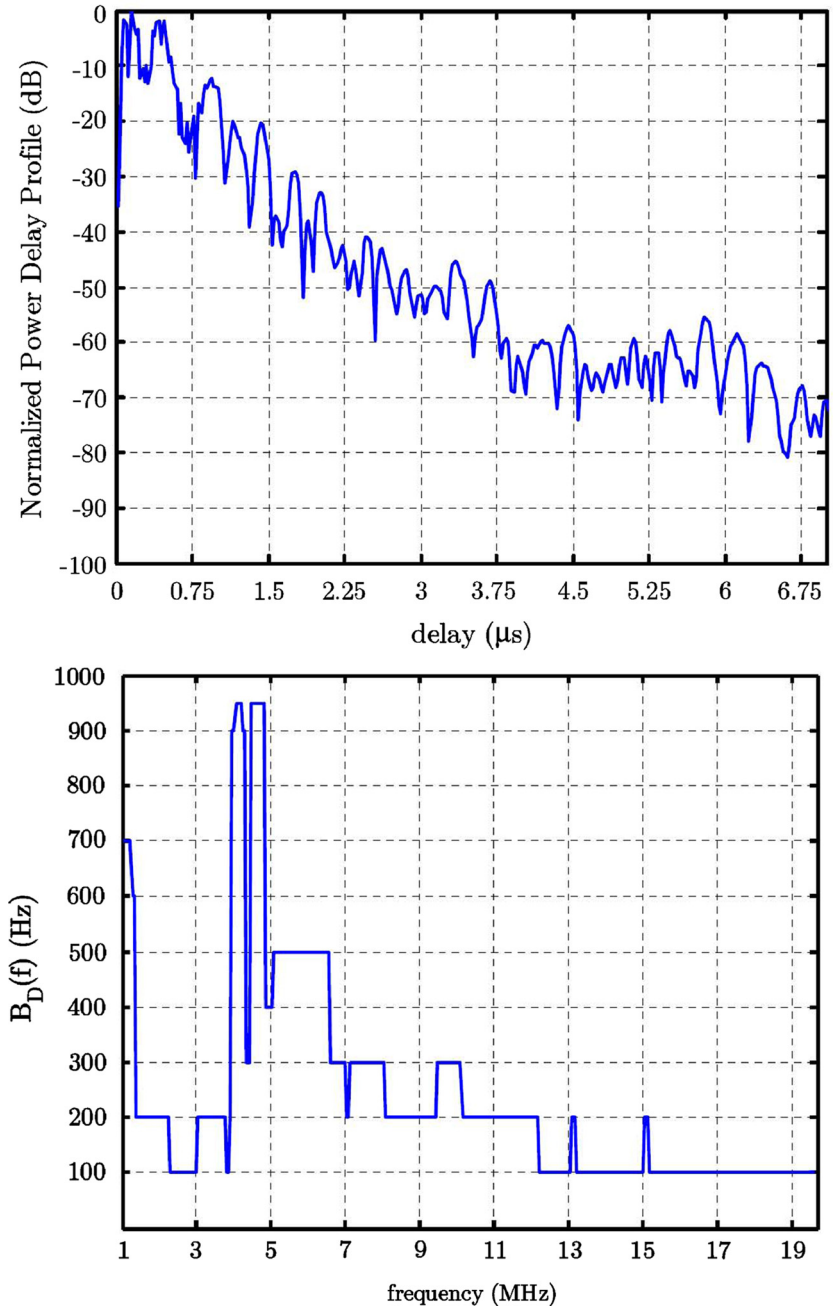

Figure 1 PDP and Doppler spread of the example channel. **(a)** Power Delay Profile; **(b)** Doppler spread.

where D accounts for the delay introduced by the synchronization process performed at the receiver. Its objective is to ensure that the DFT is computed over the set of samples in which the distortion from the previous and successive symbols is minimal [24]. The receiver will set $D = 0$ when a sufficient cyclic prefix is employed, since in this case the useful part of the OFDM symbols has no trace of the previous and successive symbols.

Subsequent expressions can be simplified by separating the impulse response of the channel during the useful part of the ℓth symbol (i.e., excluding the cyclic prefix) in two terms,

$$h[n + \ell L + cp + D, m] = h_\ell[m] + \Delta h_\ell^n[m] \quad 0 \le n \le N - 1, \quad (6)$$

where $h_\ell[m]$ is the impulse response at the middle of the useful part of the ℓth OFDM symbol and $\Delta h_\ell^n[m]$ accounts for the time variation of the channel during the nth sample of the ℓth symbol with respect to $h_\ell[m]$.

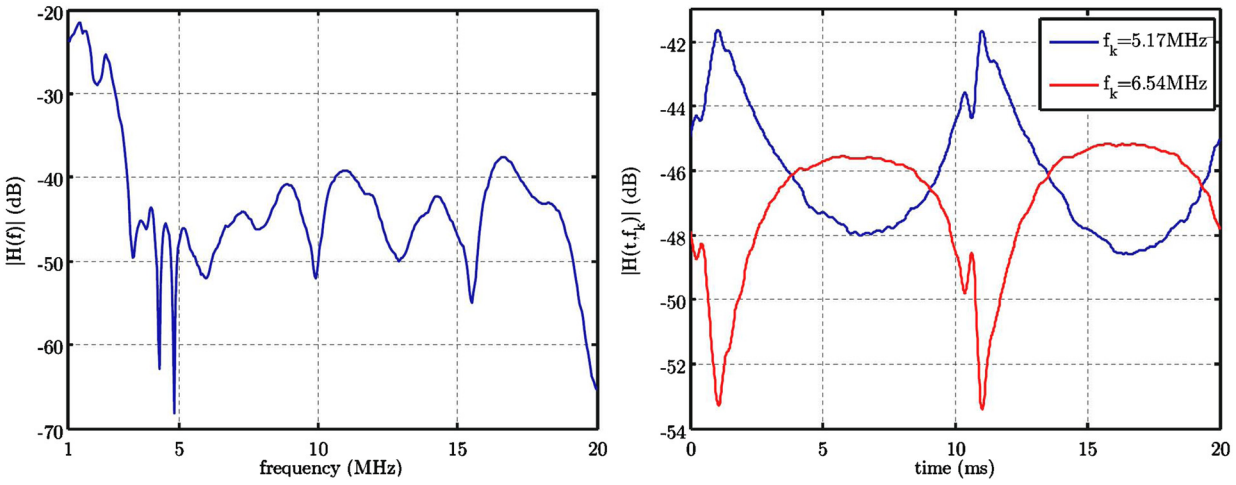

Figure 2 Frequency profile and time variation of the example channel. **(a)** Time-averaged value of the attenuation along the mains cycle; **(b)** Time evolution of the amplitude response along the mains cycle at two frequencies.

Introducing (3), (4) and (6) in (5) yields

$$Y_{\ell,k} = \sum_{q=-\infty}^{\infty} \sum_{i=-N/2+1}^{N/2} X_{q,i} \frac{e^{j\frac{2\pi}{N}i[D+(\ell-q)L]}}{N} \sum_{n=0}^{N-1} \sum_{m=0}^{L_h-1} \left(h_\ell[m] + \Delta h_\ell^n[m]\right) w_{(\ell-q)}[n-m] e^{-j\frac{2\pi}{N}im} e^{j\frac{2\pi}{N}(i-k)n}, \tag{7}$$

where for the sake of clarity, $w_{(\ell - q)}[n - m] = w[n - m + cp + D + (\ell - q)L]$ is introduced.

The inner bracket in the r.h.s. of (7) contains two terms: $h_\ell[m]$ and $\Delta h_\ell^n[m]$. The former is time-invariant during each symbol and is the responsible for the distortion due to the frequency selectivity that appears when an insufficient cyclic prefix is employed. A simplified procedure for the calculation of this distortion is proposed in Section 3.1. The latter, $\Delta h_\ell^n[m]$, varies along each OFDM symbol, which causes ICI even when a sufficient cyclic prefix is employed. A compact analytical expression for this ICI is derived in Section 3.2.

3.1. Distortion due to the channel frequency selectivity

This section is focused on the calculation of the ISI and ICI due to the frequency selectivity of the channel. Hence, the channel time variation along the OFDM symbol is disregarded, i.e., $\Delta h_\ell^n[m] = 0$. When a sufficient cyclic prefix is employed under these circumstances, expression (7) reduces to $Y_{\ell,k} = X_{\ell,k} H_\ell[k]$. This would avoid distortion but leading to an unbearable data rate penalty because of the long impulse response of power-line channels.

The key assumption to simplify the calculation of the ISI and ICI that appears when $cp < L_h - 1$ is that their magnitude is almost time-invariant. Certainly, since $h_\ell[n]$ changes from symbol-to-symbol, so does the ISI and ICI terms. However, their magnitude is mainly determined by the part of the channel impulse response not covered by the cyclic prefix [24]. Moreover, it has been shown that the delay spread of PLC channels is almost time-invariant [19]. Consequently, the energy of the remaining part of the channel impulse response (the one not included in the delay spread) would also be almost time-invariant. Therefore, if the cyclic prefix length is larger than the delay spread (as it happens in PLC), it seems reasonable to assume that the power of the distortion due to the frequency selectivity would also be almost time-invariant. This end will be corroborated *a posteriori* in Section 4 and allows calculating the ISI and ICI caused by the frequency selectivity using a time-invariant channel, $h[n]$. The impulse response of this channel can be obtained, for instance, by taking one of the impulse responses exhibited by the channel along the mains cycle. The averaged channel response along the mains cycle may also be appropriate for this purpose.

In addition, the number of carriers of interest ($N > 256$) and the considered frequency band lead to OFDM symbol lengths larger than the channel impulse response. This constrains the distortion suffered by the ℓth symbol to the ICI created by itself and to the ISI and ICI created by the previous, $(\ell - 1)$th, and the subsequent, $(\ell + 1)$th, symbols. Under these circumstances, a semi-analytical expression for the distortion can be obtained by following a similar procedure to the one in [25]. Substituting $h_\ell[n]$ by $h[n]$ and denoting $b_i[n] = h[n] * \left(w[n] e^{j\frac{2\pi}{N}i(n-cp)}\right)$, where * represents the convolution, (7) can be written as

$$Y_{\ell,k} = \sum_{i=-N/2+1}^{N/2} \left(X_{\ell,i}\, T_{\ell,i}(k) + X_{(\ell-1),i}\, T_{(\ell-1),i}(k) + X_{(\ell+1),i}\, T_{(\ell+1),i}(k)\right), \tag{8}$$

with

$$\begin{aligned} T_{\ell,i}(k) &= \frac{1}{N}\mathrm{FFT}(b_i[n+cp+D],N,k),\\ T_{(\ell-1),i}(k) &= \frac{1}{N}\mathrm{FFT}(b_i[n+cp+D-L],N,k),\\ T_{(\ell+1),i}(k) &= \frac{1}{N}\mathrm{FFT}(b_i[n+cp+D+L],N,k), \end{aligned} \tag{9}$$

and where $FFT(x[n],N,k)=\sum_{n=0}^{N-1}\mathrm{x}[n]e^{-j\frac{2\pi}{N}kn}$.

Fixing the frequency equalizer (FEQ) in carrier k to $H^{-1}[k]e^{-j\frac{2\pi}{N}kD}$, assuming equal power constellations centered in the origin and with independent data values, the signal-to-distortion ratio[a] (SDR) due to the frequency selectivity (FS) in carrier k may be obtained as

$$\begin{aligned} SDR_{FS}(k) &= \frac{E\left[|X_{\ell,k}|^2\right]}{E\left[|X_{\ell,k}-Y_{\ell,k}FEQ(k)|^2\right]}\\ &= \frac{|H[k]|^2}{ISI(k)+ICI(k)+|H(k)e^{j\frac{2\pi}{N}kD}-T_{\ell,k}(k)|^2}, \end{aligned} \tag{10}$$

where

$$ISI(k)=|T_{(\ell-1),k}(k)|^2+|T_{(\ell+1),k}(k)|^2, \tag{11}$$

$$\begin{aligned} ICI(k) = \sum_{\substack{\mathrm{i}=-\mathrm{N}/2+1\\ i\neq k}}^{N/2} &(|T_{(\ell-1),i}(k)|^2+|T_{\ell,i}(k)|^2\\ &+|T_{(\ell+1),i}(k)|^2). \end{aligned}$$

In addition to the ISI and ICI terms, the denominator in the r.h.s. of (10) contains a third distortion term. It reflects that the output symbol can no longer be expressed as $Y_{\ell,k}=X_{\ell,k}H[k]e^{j\frac{2\pi}{N}kD}$ when an insufficient cyclic prefix is employed, not even in the case of a one-shot transmission using one single carrier.

Alternatively, the term $\mathrm{SDR}_{\mathrm{FS}}(k)$ can be estimated by means of simple simulations. Using a state-of-the-art computer, this strategy has proved to be faster than the proposed semi- analytical method when the number of carriers is approximately $N > 2^{14}$.

3.2. Distortion due to the channel time variation

To calculate this distortion term, the cyclic prefix length can be fixed to the most convenient value, e.g., $cp \geq L_h - 1$. The reason is that the ICI generated by the channel time variation is almost independent of the cyclic prefix, since the latter is discarded before the DFT computed at the receiver. Hence, only the time variation of the channel along the useful part of the OFDM symbols is reflected at the output of the DFT. By selecting $cp \geq L_h - 1$, it is ensured that distortion terms due to the channel frequency selectivity are eliminated, what simplifies the problem. Certainly, the time variation of the channel during the preceding and subsequent symbols cause additional distortion when $cp < L_{h-1}$, but it is negligible when compared with the remaining terms. Fixing $cp \geq L_h - 1$ (and $D = 0$), expression (7) can be expressed as

$$\begin{aligned} Y_{\ell,k} = X_{\ell,k}H_\ell[k] &+ \frac{1}{N}\sum_{i=-N/2+1}^{N/2} X_{\ell,i}\\ &\times\sum_{n=0}^{N-1}\left(\sum_{m=0}^{L_h-1}\Delta h_\ell^n[m]e^{-j\frac{2\pi}{N}im}\right)e^{j\frac{2\pi}{N}(i-k)n}, \end{aligned} \tag{12}$$

where

$$H_\ell[k]=\sum_{m=0}^{L_h-1}h_\ell[m]e^{-j\frac{2\pi}{N}km}. \tag{13}$$

For the number of carriers in the range of interest, the channel can be assumed to have a slow-varying behavior, and its variation along the useful part of the OFDM symbol may be approximated as linear [26]

$$\Delta h_\ell^n[m]\approx\Delta h_\ell[m]\frac{(n-N/2+1/2)}{N}\quad 0\leq \mathrm{n}\leq N-1, \tag{14}$$

where $\Delta h_\ell[m]$ denotes the difference in the value of the impulse response from the beginning to the end of the symbol. The range of validity of this approximation will be assessed, *a posteriori*, in Section 4.

Introducing (14) into (12) results in

$$\begin{aligned} Y_{\ell,k} = X_{\ell,k}H_\ell[k] &+ j\frac{1}{2N}\sum_{\substack{i=-N/2+1\\ i\neq k}}^{N/2} X_{\ell,i}\Delta H_\ell[i]\\ &\times\frac{e^{-j\frac{\pi}{N}(i-k)}}{sin\left(\frac{\pi}{N}(i-k)\right)}, \end{aligned} \tag{15}$$

where

$$\Delta H_\ell[k]=\sum_{m=0}^{L_h-1}\Delta h_\ell[m]e^{-j\frac{2\pi}{N}km}. \tag{16}$$

As seen, the second term in the r.h.s. of (15) is the ICI due to the channel time variation.

Since the channel response variation is periodic, it is interesting to consider an OFDM system in which transmissions are synchronized with the mains signal. This strategy provides important data rate gains because it allows exploiting the periodical behavior of the SNR [27]. Assuming that P-complete OFDM symbols can be fitted into each mains period, the symbol index, ℓ, can be expressed as $\ell = p + rP$, where $0 \leq p \leq P - 1$ and $-\infty < r < \infty$. Then, due to the periodic behavior of the channel, it holds that $H_{p+rP}[m] = H_p[m]$ and $\Delta H_{p+rP}[m] = \Delta H_p[m]$.

By setting the FEQ in carrier k to $H_p^{-1}[k]$ and using zero-mean equal power constellations with independent

data values, the SDR due to the channel time variations (TV) in carrier k can be expressed as

$$\mathrm{SDR}_{\mathrm{TV}}(p,k) = \frac{E[|X_{p,k}|^2]}{E[|X_{p,k}-Y_{p,k}H_p^{-1}[k]|^2]} = \frac{4N^2|H_p[k]|^2}{\sum_{\substack{i=-N/2+1 \\ i\neq k}}^{N/2} \frac{|\Delta H_p[i]|^2}{\sin^2\left(\frac{\pi}{N}(i-k)\right)}}. \quad (17)$$

It should be noted that the expectation in (17) is performed over the data values, $X_{p,\,k}$, since the channel response is deterministic once the transmitter and receiver locations are fixed.

3.3. Overall distortion calculation

According to (8) and (15), the output of the DFT performed at the receiver can be expressed as

$$Y_{\ell,k} = X_{\ell,k}\, T_{\ell,k}(k) + \sum_{\substack{i=-N/2+1 \\ i\neq k}}^{N/2} X_{\ell,i} T_{\ell,i}^{TV}(k) + \sum_{\substack{i=-N/2+1 \\ i\neq k}}^{N/2} X_{\ell,i}\, T_{\ell,i}(k) + \sum_{i=-N/2+1}^{N/2} (X_{(\ell-1),i} T_{(\ell-1),i}(k) + X_{(\ell+1),i} T_{(\ell+1),i}(k)), \quad (18)$$

where

$$T_{\ell,i}^{TV}(k) = \frac{j}{2N}\Delta H_\ell[i] \frac{e^{-j\frac{\pi}{N}(i-k)}}{\sin\left(\frac{\pi}{N}(i-k)\right)}. \quad (19)$$

The second term in the r.h.s. of (18) represents the distortion due to the time variation of the channel, while the third and fourth terms represent the distortion caused by the frequency selectivity. Provided that the transmitted data values are independent and zero-mean, the power of the overall distortion would be computed by summing the power of the individual terms. However, this is prevented by the fact that the second and the third ICI components are caused by the same data values. Therefore, its power is given by

$$E\left[\left|\sum_{\substack{i=-N/2+1 \\ i\neq k}}^{N/2} X_{\ell,i}[T_{\ell,i}^{TV}(k) + T_{\ell,i}(k)]\right|^2\right] = E[|X_{\ell,i}|^2] \times \left(\sum_{\substack{i=-N/2+1 \\ i\neq k}}^{N/2} [|T_{\ell,i}^{TV}(k)|^2 + |T_{\ell,i}(k)|^2] + \sum_{\substack{i=-N/2+1 \\ i\neq k}}^{N/2} 2Re[T_{\ell,i}^{TV}(k) T_{\ell,i}(k)^*]\right). \quad (20)$$

Nevertheless, it is reasonable to assume that $T_{\ell,i}^{T} V(k)$ and $T\ell,\ i(k)$ are uncorrelated because they have independent causes: the former is due to the time variation of the channel and the latter is caused by the frequency selectivity. Accordingly,

$$\sum_{\substack{i=-N/2+1 \\ i\neq k}}^{N/2} 2Re\left[T_{\ell,i}^{TV}(k) T_{\ell,i}(k)^*\right] = 0. \quad (21)$$

The validity of this assumption will be corroborated *a posteriori* in Section 4.

As a result, the overall SDR experienced by an OFDM system with *cp* samples of cyclic prefix and which transmissions are synchronized with the mains signal can be obtained by the following procedure:

(1) Estimate the SDR in carrier k due to the frequency selectivity, $\mathrm{SDR}_{\mathrm{FS}}(k)$, using a cyclic prefix of *cp* samples. This can be accomplished using (10) or by means or simulations.

(2) Calculate the SDR due to the channel time variation, $\mathrm{SDR}_{\mathrm{TV}}(p, k)$, using expression (17).

(3) Obtain the overall SDR in carrier k of the pth transmitted symbol in each mains cycle according to

$$SDR(p,k) = \left[SDR_F S(k)^{-1} + SDR_{TV}(p,k)^{-1}\right]^{-1}. \quad (22)$$

4. Method validation

Results obtained with the proposed methodology are now compared to those given by LPTV simulations. The channel extends up to 25 MHz and the carrier frequency of the OFDM system is fixed to 12.5 MHz. Hence, the sampling frequency for the baseband equivalent system is set to f_s = 25 MHz. The LPTV filtering is performed using the *direct form A* structure described in [23]. The filter bank consists of 976 filters, whose impulse responses have been obtained by sampling the channel impulse response at regularly distributed intervals within the mains cycle. These simulations involve significant computational complexity because, in practice, the calculation of each output symbol from the channel requires the use of several filters from the bank.

Firstly, the accuracy of the analytical expression derived for the ICI caused by the channel time variation is assessed. To this end, it must be ensured that there is no distortion due to the channel frequency selectivity when computing the SDR by means of LPTV simulations. This can be achieved by fixing the cyclic prefix to the extremely high value of *cp* = 511 samples (20.44 μs at 25 MHz). Figure 3 shows the time and frequency-averaged SDR values versus the base-two logarithm of the number of carriers: curve a has been obtained from (17) and curve b from LPTV simulations. As expected, the difference between both curves

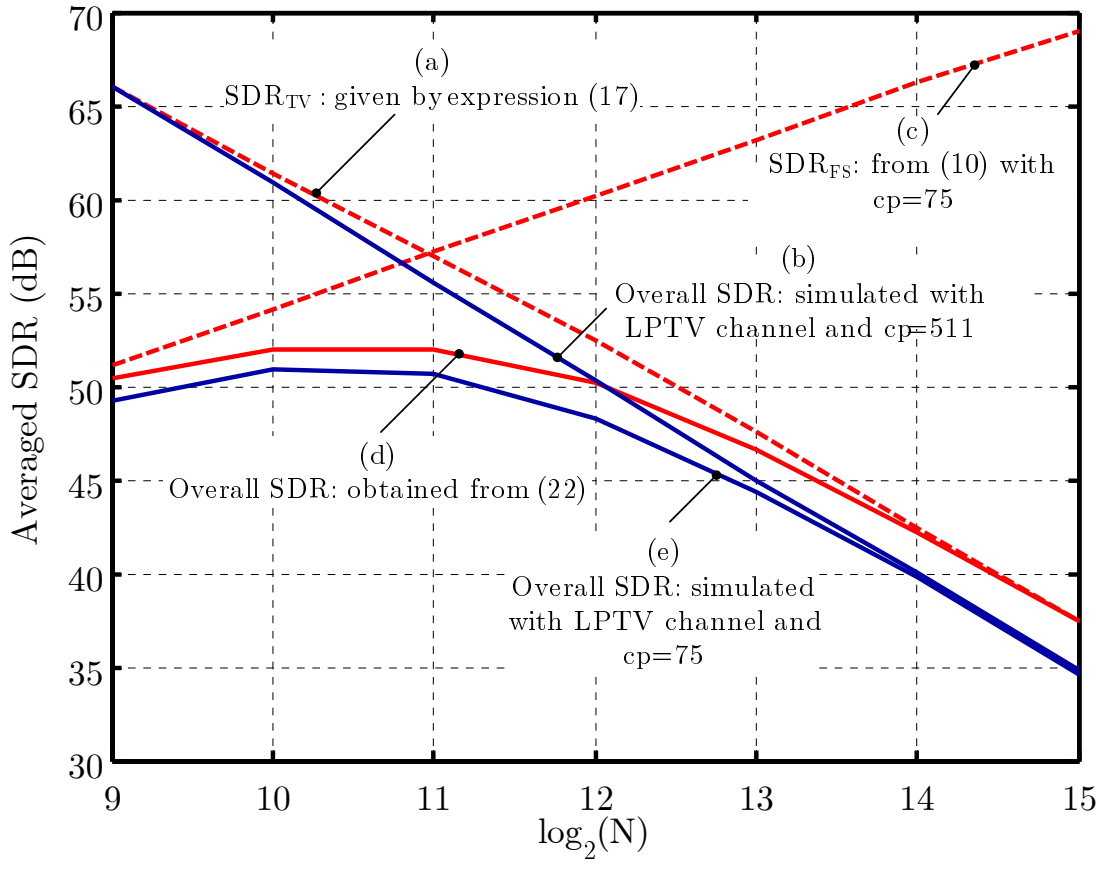

Figure 3 Averaged SDR in the selected channel.

increases with the number of carriers. The reason is that curve a has been obtained assuming that the channel impulse response has a linear variation along the OFDM symbol. Increasing the number of carriers enlarges the symbol length and, consequently, the error made by the linear approximation. However, for $N = 2^{11}$, which can be considered an upper bound in the number of carriers currently used by commercial PLC systems, the difference between curves a and b is smaller than 1.5 dB. Moreover, even for a number of carriers as high as $N = 2^{15}$, the difference is smaller than 2.6 dB. In both cases, the error is smaller than the SNR increment (3 dB) required to transmit one additional bit per symbol in an AWGN channel. In addition, it should be reminded that the considered channel is a worst case one, in terms of channel time variation. Therefore, the aforementioned errors may be taken as upper bounds.

Secondly, the suitability of (22) to calculate the overall SDR is verified. As an example, let us assume that we want to compute the overall SDR experienced when the cyclic prefix length is set to $cp = 75$ samples (3 μs at 25 MHz). The values of $SDR_{FS}(k)$ have been computed using (10) with the LTI response that results from the averaging of the impulse response exhibited by the channel along the mains cycle. Curve c in Figure 3 depicts the frequency-averaged values of the obtained results. Curve d shows the time and frequency-averaged values given by (22). Clearly, it tends to curve c in the low number of carriers region and to curve a in the high number of carriers zone. It can be seen that the differences between curves d and e, obtained by means of LPTV simulations, are smaller than 2 dB for $N \leq 2^{11}$.

The additivity of the distortion due to the frequency selectivity and to the time variation of the channel can also be corroborated by concentrating in the SDR values for $N = 2^{11}$, where the power of both terms is similar. As seen, the difference between curve d, which assumes additivity, and curve e, which makes no assumption, is about 1.4 dB. However, this error is almost exclusively due to the linear variation approximation employed to obtain curve d. This can be verified just by noting that 1.4 dB is the error between curve a, which uses the linear variation approximation but in which there is only one distortion term, and curve b, which makes no approximation and which there is also only one distortion term.

Finally, results presented in Figure 3 are also used to assess the validity of the time-invariant behavior assumed for

the distortion caused by the channel frequency selectivity. To this aim, let us concentrate in the region where $N \leq 2^{10}$, in which the distortion due to the frequency selectivity is the dominating term, as can be easily observed by comparing curves a and c. Differences between the overall SDR estimated with the proposed method, shown in curve d, and the one computed by means of simulations, depicted in curve e, are smaller than 1.3 dB. The negligible effect of the ICI due to the channel time variation in this zone allows concluding that this divergence is due to the time-variant magnitude of the ISI and ICI caused by the frequency selectivity.

5. Performance analysis

Performance evaluation presented in this section is accomplished over the set of measured channels introduced in Section 2. As mentioned in Section 1, it is inappropriate to assess the performance of the OFDM system in terms of the SNIR, since maximizing it does not maximizes the bit-rate. The reason is that the system bit-rate has a direct dependence on both the SNIR and the symbol rate. Since PLC channel responses are quite long, enlarging the cyclic prefix improves the SNIR but reduces the symbol rate. This motivates the use of the bit-rate as the system performance indicator.

However, obtaining the bit-rate subject to a certain objective bit error rate (BER) requires the knowledge of the probability distribution of the noise and the distortion. Since there is no accepted statistical model for the PLC channel response, the distribution of the distortion is unknown. Nevertheless, we can assume that they are gaussianly distributed to obtain a lower bound for the bit-rate. This is the approach followed in this section.

5.1. Bit-rate calculation

One of the advantages of OFDM is that the constellation employed in each carrier can be selected according to its particular channel conditions. Moreover, these constellations can also be changed with time. The objective is to transmit at high data rates when channel conditions are favorable and to reduce the throughput when the channel gets poorer, while guaranteeing a target BER.

In an actual channel, the output of the DFT performed at the receiver can be written as

$$Y_{p,k} = X_{p,k}H_p[k] + N_{p,k} + D_{p,k}, \tag{23}$$

where $N_{p,\,k}$ and $D_{p,\,k}$ are the cyclostationary noise and distortion terms, respectively. The signal-to-noise and distortion ratio (SNDR)[b] can then be defined as

$$\mathrm{SNDR}(p,k) = \frac{E[|X_{p,k}|^2]}{E[|X_{p,k} - Y_{p,k}H_p^{-1}[k]|^2]}, \tag{24}$$

assuming that the noise and the distortion are independent, and denoting their respective power as $\sigma^2_{N_{p,k}}$ and $\sigma^2_{D_{p,k}}$, and the signal power by $\sigma^2_{X_{p,k}}$, the SNDR can be expressed as

$$\begin{aligned}\mathrm{SNDR}(p,k) &= \frac{\sigma^2_{X_{p,k}}}{\left|H_p^{-1}[k]\right|^2\left(\sigma^2_{N_{p,k}} + \sigma^2_{D_{p,k}}\right)} \\ &= \left[\frac{\sigma^2_{N_{p,k}}}{\left|H_p[k]\right|^2\sigma^2_{X_{p,k}}} + \frac{\sigma^2_{D_{p,k}}}{\left|H_p[k]\right|^2\sigma^2_{X_{p,k}}}\right]^{-1} \\ &= \left[\mathrm{SNR}(p,k)^{-1} + \mathrm{SDR}(p,k)^{-1}\right]^{-1}\end{aligned} \tag{25}$$

where SDR(p, k) is computed according to (22) and SNR (p, k) denotes the SNR in carrier k of the pth symbol transmitted in each mains cycle, which can easily be computed from the transmitter power spectral density (PSD) and the instantaneous PSD of the cyclostationary noise.

Hence, the OFDM system can be seen as a set of $P \times N$ independent channels. Assuming that both the noise and the distortion have a Gaussian distribution, the number of bits per symbol that can be transmitted in carrier k during the pth symbol of each mains cycle is given by the simple expression

$$b(p,k) = \left\lfloor \log_2\left(\frac{1 + \mathrm{SNDR}(p,k)}{\Gamma}\right)\right\rfloor, \tag{26}$$

where Γ is the so-called *SNR gap* and models the SNR penalty experienced because of the use of a discrete constellation. For square QAM constellations, it can be approximated by [28]

$$\Gamma = -\frac{1}{1.6}\ln\left(\frac{\mathrm{BER}_{\mathrm{obj}}}{0.2}\right), \tag{27}$$

where $\mathrm{BER}_{\mathrm{obj}}$ is the objective BER constraint.

The bit-rate achieved when employing N carriers and cp samples of cyclic prefix can then be obtained according to

$$R(N,cp) = \frac{f_s}{(N+cp)\times P}\sum_{p=0}^{P-1}\sum_{k=0}^{N-1} b(p,k), \tag{28}$$

where f_s is the sampling frequency and denotes P the number of OFDM symbols in each mains cycle.

5.2. Selection of the modulation parameters

A performance criterion must be defined to select the modulation parameters. The most straightforward is to maximize the aggregate bit-rate of the set considered channels. However, the significant SNDR differences between PLC channels may lead to the quite unfair situation in which the most appropriate parameters are practically equal to the ones that maximize the bit-rate in the channel with the highest SNDR values. To avoid this, a different criterion is employed in this study. It

begins by computing the bit-rate loss caused by the use of a non-optimum cyclic prefix in the mth channel

$$\alpha_m(N, cp) = 1 - \frac{R_m(N, cp)}{\max\limits_{N,cp}\{R_m(N, cp)\}}, \quad (29)$$

where $R_m(N, cp)$ is the bit-rate achieved in the mth channel. Denoting by M the number of channels employed in the analysis (which exceeds 50) the averaged bit-rate loss over the set of considered channels is then calculated as [9]

$$\overline{\alpha}(N, cp) = \frac{1}{M}\sum_{m=1}^{M}\alpha_m(N, cp). \quad (30)$$

This parameter is now used as a performance indicator to determine the most appropriate values for the number of carriers and cyclic prefix length. The transmitter PSD is fixed to -20 dBm/kHz, which is in accordance with the PSD mask fixed by the upcoming ITU Rec. G.9960. BPSK and square QAM constellations subject to an objective BER of 10^{-3} are employed. Constellations with up to 12 bits per symbol are employed. The number of carriers is varied in a range of up to $N = 2^{15}$, which is much higher than the ones employed in state-of-the-art modems. This allows exploring the theoretical limits of the modulation, rather than constraining it to the current state of technology.

Figure 4a depicts the values in (30) expressed as a percentage. Detailed results for representative cyclic prefixes are shown in Figure 4b. As expected, the cyclic prefix length has a strong influence in the performance only when the number of carriers is low. In these situations, distortion due to the frequency selectivity is the limiting term, and a careful selection of the cyclic prefix must be performed. On the other hand, distortion due to the time variation becomes the dominating term when the number of carriers increases and, except for very low values of the cyclic prefix, the influence of the cyclic prefix is very small. This can be clearly observed in Figure 4b, where a *cp* variation of 100 samples results in a performance variation smaller than 1.5% for $N \geq 2^{11}$. According to this, Table 1 shows approximate values of the optimum cyclic prefix lengths. It can also be observed that the most appropriate number of carriers is $N = 2^{13}$, although the averaged bit-rate loss is still below 3.5% for $N = 2^{12}$. In a 25 MHz frequency band, $N = 2^{13}$ results in a carrier bandwidth of 3.1 kHz. This value is much lower than the one employed by current commercial system, which is in the order of 24.4 kHz [7]. Hence, considerable performance improvements can still be achieved just by increasing the number of carriers.

Table 1 Approximate values of the optimum cyclic prefix length (at 25 MHz) as a function of the number of carriers

N	2^9	2^{10}	2^{11}	2^{12}	2^{13}	2^{14}	2^{15}
cp (Samples)	50	75	75	125	150	175	200

Results presented in Figure 4b can be used to determine the most appropriate number of carriers. However, to decide the value to be used in a practical system, it would be useful to know the absolute values of the bit-rate. This will allow evaluating whether the bit-rate gain compensates for the increment in the implementation complexity. Figure 5 shows the maximum, the mean, and the minimum values of the bit-rate (computed over the set of considered channels) as a function of the number of carriers. The cyclic prefix values given in Table 1 have employed. As seen, moving from $N = 2^9$ to $N = 2^{11}$ boosts the mean value of the bit-rate from approximately 119 up to 137.2 Mbit/s. However, subsequent increments provide reduced gains, e.g., the mean value of the bit-rate for $N = 2^{13}$ is 139.2 Mbit/s. Similar conclusions can be drawn for the maximum and the minimum bit-rate values.

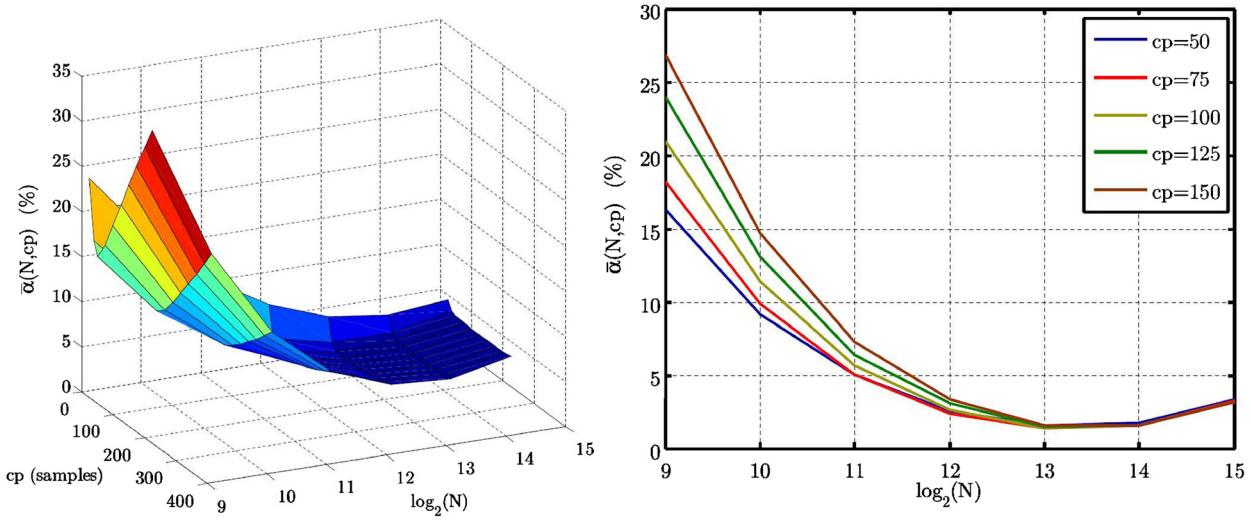

Figure 4 Averaged bit-rate loss over the set of considered channels. **(a)** Averaged bit-rate loss as a function of the number of carriers and the cyclic prefix length; **(b)** Averaged bit-rate loss for selected cyclic prefix lengths.

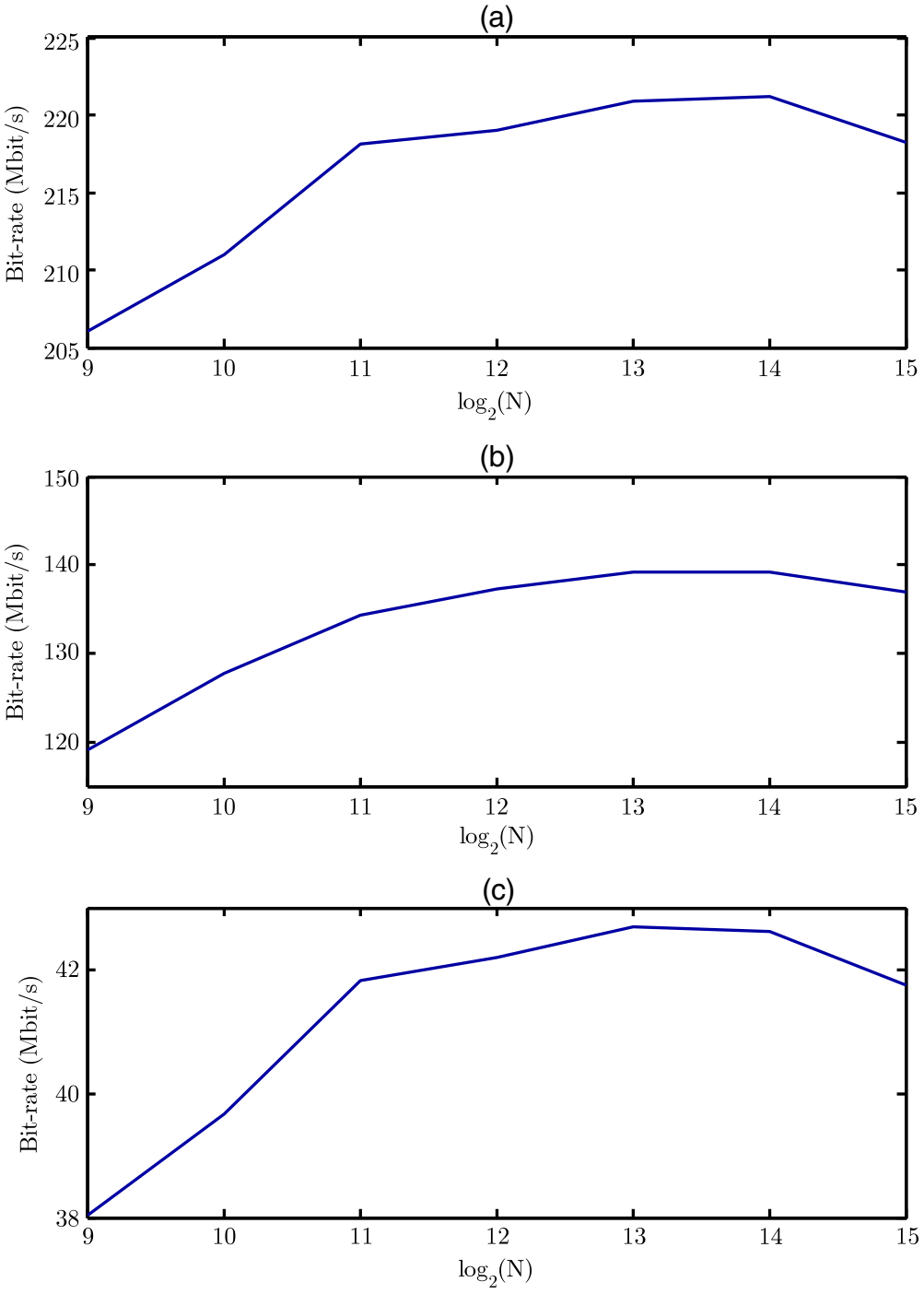

Figure 5 Bit-rate values of the set of considered channels as a function of the number of carriers. **(a)** Maximum, **(b)** mean, and **(c)** minimum.

6. Conclusion

This article has presented a new method to compute the distortion suffered by OFDM signals on indoor broadband power-line channels. The overall distortion is the sum of two terms: one due to the frequency selectivity and another caused by the channel time variation. It has been shown that the former is almost time-invariant and, hence, can be computed using an LTI filter. The latter is calculated by means of a novel analytical expression that, due to the periodically variant nature of

the channel, has a particularly compact expression. These results have been used to assess the performance of the OFDM modulation on a set of measured indoor power-line channels. Optimum values for the cyclic prefix length and the number of carriers have been given.

Endnotes

[a]The SDR is also referred to as SIR, where the term interference refers to the ISI and ICI.

[b]The SNDR is sometimes referred to as signal to interference and noise ratio (SINR), where the term interference refers to the ICI and ISI, and also as SNR, where the term noise refers to all the unwanted components, i.e., the channel noise and the distortion.

Acknowledgements

This study was partially supported by the Spanish MEC under Project TIC2003-06842. The authors would like to thank the anonymous reviewers for their valuable comments and suggestions.

Competing interests

The authors declare that they have no competing interests.

Received: 23 December 2010 Accepted: 27 September 2011
Published: 27 September 2011

References

1. ITU-T Recommendation G.9960, Next generation home networking transceivers
2. V Oksman, S Galli, G.hn: the new ITU-T home networking standard. IEEE Commun Mag. **47**, 138–145 (2009)
3. ETSI, Powerline telecommunications (PLT). Coexistence of access and in-house powerline systems, in *TS 101 867 V1.1.1*, (2000)
4. H Philipps, Performance measurements of power-line channels at high frequencies, in *Proceedings of the International Symposium on Power Line Communications and its Applications (ISPLC)*, 229–237 (1998)
5. FJ Cañete, JA Cortés, L Díez, JT Entrambasaguas, Analysis of the cyclic short-term variation of indoor power line channels. IEEE J Sel Areas Commun. **24**(7), 1327–1338 (2006)
6. M Lee, R Newman, H Latchman, S Katar, L Yonge, Homeplug 1.0 powerline communication LANs-protocol description and performance results. Int J Commun Syst. **16**(5), 447–473 (2003). doi:10.1002/dac.601
7. Homeplug, HomePlug AV White Paper. Homeplug Tech Rep (2005)
8. AM Tonello, S D'Alessandro, L Lampe, Cyclic prefix design and allocation in bit-loaded OFDM over power line communication channels. IEEE Trans Commun. **58**(11), 1–12 (2010)
9. JJ Sánchez-Martínez, JA Cortés, L Díez, FJ Cañete, LM Torres, Performance analysis of OFDM modulation on indoor PLC channels in the frequency band up to 210 MHz, in *Proceedings of the IEEE International Symposium on Power Line Communications and Its Applications (ISPLC)* (2010)
10. M Russel, GL Stüber, Interchannel interference analysis of OFDM in a mobile environmnent, in *Proceedings of the IEEE VTC*, 820–824 (1995)
11. H Steendam, M Moeneclaey, Analysis and optimization of the performance of OFDM on frequency-selective time-selective fading channels. IEEE Trans Commun. **47**(12), 1811–1819 (1999). doi:10.1109/26.809701
12. FJ Cañete, JA Cortés, L Díez, JT Entrambasaguas, Modeling and evaluation of the indoor power line channel. IEEE Commun Mag. **41**(4), 41–47 (2003). doi:10.1109/MCOM.2003.1193973
13. Y Mostofi, DC Cox, ICI mitigation for pilot-aided OFDM mobile systems. IEEE Trans Wirel Commun. **4**, 765–774 (2005)
14. Y-S Choi, PJ Voltz, F Cassara, On channel estimation and detection for multicarrier signals in fast and frequency selective rayleigh fading channel. IEEE Trans Commun. **49**, 1375–1387 (2001). doi:10.1109/26.939860
15. L Wan, VK Dubey, Bit error probability of OFDM system over frequency nonselective fast Rayleigh fading channels. Electron Lett. **36**, 1306–1307 (2000). doi:10.1049/el:20000944
16. K Kim, H Park, H-R You, Parameters optimization of multiuser OFDM on doubly selective fading channels, in *Proceedings of the IEEE Vehicular Technology Conference (VTC)*, 933–937 (May 2008)
17. E Biglieri, S Galli, Y-H Lee, HV Poor, AJ Han Vinck, Guest editorial. *IEEE Journal on Selected Areas on Communications* **24**, 1261–1264 (2006)
18. S Galli, TC Banwell, A deterministic frequency-domain model for the indoor power line transfer function. IEEE J Sel Areas Commun. **24**(7), 1304–1316 (2006)
19. JA Cortés, FJ Cañete, L Díez, JT Entrambasaguas, Characterization of the cyclic short-time variation of indoor power-line channels response, in *Proceedings of the International Symposium on Power Line Communications and its Applications (ISPLC)*, 326–330 (2005)
20. JA Cortés, L Díez, FJ Cañete, JJ Sánchez-Martínez, Analysis of the indoor broadband power-line noise scenario. IEEE Trans Electromag Compatib. **52**(4), 849–858 (2010)
21. FJ Cañete, JA Cortés, L Díez, JT Entrambasaguas, A channel model proposal for indoor power line communications. IEEE Commun Mag (2010)
22. JG Proakis, *Digital Communications* (McGraw-Hill, 1995)
23. SM Phoong, PP Vaidyanathan, Time-varying filters and filter banks: some basic principles. IEEE Trans Signal Process. **44**(12), 2971–2987 (1996). doi:10.1109/78.553472
24. T Pollet, M Peeters, Synchronization with DMT modulation. IEEE Commun Mag. **37**(4), 80–86 (1999). doi:10.1109/35.755454
25. JA Cortés, L Díez, FJ Cañete, JT Entrambasaguas, Analysis of DMT-FDMA as a multiple access scheme for broadband indoor power-line communications. IEEE Trans Consum Electron. **52**(4), 1184–1192 (2006)
26. JA Cortés, L Díez, FJ Cañete, JT Entrambasaguas, Distortion evaluation of DMT signals on indoor broadband power-line channels, in *Proceedings of the Third International Workshop on Power Line Communications (WSPLC)*, Udine, Italy, (2009)
27. S Katar, B Mashburn, K Afkhamie, H Latchman, R Newman, Channel adaptation based on cyclo-stationary noise characteristics in PLC systems, in *Proceedings of the IEEE International Symposium on Power Line Communications and its Applications (ISPLC)*, 16–21 (March 2006)
28. ST Chung, AJ Goldsmith, Degrees of freedom in adaptive modulation: a unified view. IEEE Trans Commun. 49(9), 1561–1571 (2001). doi:10.1109/26.950343

doi:10.1186/1687-6180-2011-78
Cite this article as: Cortés *et al.*: **Performance analysis of OFDM modulation on indoor broadband PLC channels.** *EURASIP Journal on Advances in Signal Processing* 2011 **2011**:78.